Volume 11, Issue 7, July – 2026 International Journal of Innovative Science and Research Technology
ISSN No:-2456-2165 https://doi.org/10.38124/ijisrt/26jul270

Electrical Conduction in $Ba_{0.835}Ca_{0.165}Zr_{0.09}Ti_{0.91}O_3$ Ceramic

Himanshi Kumari[1]; Ram Kumar[1]; Sandeep K. Jha[1]; Abhishek Kumar[1]; Kumar P. Chandra[2]; Ajit R. Kulkarni[3]; K. Prasad[1]

[1]University Department of Physics, T.M. Bhagalpur University, Bhagalpur 812007, India
[2]Department of Physics, S. M. College, Bhagalpur 812001, India
[3]Department of Metallurgical Engineering and Materials Science, Indian Institute of Technology, Mumbai 400076, India

Publication Date: 2026/07/22

Abstract: High dielectric constant materials are gaining significant attention due to their increasing demand in critical sectors such as aerospace, aeronautics, power generation, and the automotive industry. This work undertakes the structural, microstructural, dielectric, and AC conductivity studies of the ceramic system $Ba_{0.835}Ca_{0.165}Zr_{0.09}Ti_{0.91}O_3$, synthesized via the conventional mixed oxide reaction process. X-ray diffraction analysis ascertained the formation of a perovskite-type tetragonal structure having the space group *P4/mmm*. The average grain size of the ceramic was estimated to be ~6 µm. At room temperature and 1 kHz, the dielectric constant and tangent loss were obtained to be 4351 and 0.015, respectively. Besides, the dielectric capacitor exhibited a resonance frequency above 0.66 MHz at 800°C that shifted to 0.16 MHz at 850°C. AC conductivity analysis suggests a hopping-type charge transport mechanism, consistent with the jump relaxation model, and an apparent activation energy of 0.66 eV at 1 Hz. These results indicated the potential of the present lead-free ceramic material for future industrial applications.

Keywords: *Ceramic; Lead Free; Solid-State Reaction; Dielectric Constant; Phase Transition; Electrical Conduction.*

How to Cite: Himanshi Kumari; Ram Kumar; Sandeep K. Jha; Abhishek Kumar; Kumar P. Chandra; Ajit R. Kulkarni; K. Prasad (2026) Electrical Conduction in $Ba_{0.835}Ca_{0.165}Zr_{0.09}Ti_{0.91}O_3$ Ceramic. *International Journal of Innovative Science and Research Technology*, 11(7), 578-583. https://doi.org/10.38124/ijisrt/26jul270

I. INTRODUCTION

Materials with exceptionally high dielectric constants have garnered ample concern in the recent past, largely because of their growing demand in aerospace, aeronautics, automotive sectors, and power generation industries. These applications generally involve ferroelectric devices operating under extreme conditions and wide temperature ranges, including high-end areas like space exploration, aerospace propulsion systems, turbines and fans operated at high temperature, combustion monitoring sensors, engines, and actuators [1-3]. Moreover, high-temperature ferroelectric substances have found their use in specialized fields such as valve control in oil and natural gas extraction, non-destructive assessment of crucial nuclear appliances, and systems of thermal as well as geothermal engineering [4]. Despite the need, only a limited number of compounds have been explored for their applications in high-temperature areas. These include $GaPO_4$, $LiNbO_3$, SiO_2, AlN, $La_3Ga_5SiO_{14}$, $CaZrO_3$–$Bi_{1/2}Na_{1/2}TiO_3$, and rare-earth borates like $ReCa_4O(BO_3)_3$ (Re = Gd, La, Y), among others [5-15]. Further, certain Fe-containing compounds such as $A(Fe_{1/2}B_{1/2})O_3$ (here A = Ca, Sr, Ba; B = Ta, Nb, Sb) have also received interest for their colossal dielectric behavior ($\varepsilon \approx 10^3$–10^5) across wide temperature as well as frequency ranges, like that of $CaCu_3Ti_4O_{12}$ [2,16-25]. Recent studies have suggested bismuth-based materials such as $BiFeO_3$ and $Bi_4Ti_3O_{12}$ display high transition temperatures (600–800°C). However, their application is limited by a narrow processing window and the necessity for precise doping. In an effort to overcome such limitations, a novel modified barium titanate-based ferroelectric solid-solution, $(1\text{-}x)(Ba_{0.7}Ca_{0.3})TiO_3$–$xBa(Zr_{0.2}Ti_{0.8})O_3$ (BCT-BZT) that features a morphotropic phase boundary (MPB) at x = 0.50 has been proposed [26]. This composition displays a triple point (cubic-rhombohedral-tetragonal), offering a dielectric constant ($\varepsilon \approx 3060$) and a notable piezoelectric coefficient ($d_{33} \approx 620$ pC/N) [26], akin to the soft $Pb(Zr,Ti)O_3$-based ceramics that are available commercially. However, the phase-transition of this solid-solution occurs at ~90°C is relatively low for high-temperature applications. To date, limited studies, primarily from the authors' group [27–29], have explored the behavior of BCT-BZT ceramics at elevated temperatures (> 500°C), which has become the motivation behind this research. Furthermore, understanding the electrical conductivity in such materials is crucial, as it directly influences their physical properties and poling strategies. Therefore, an in-depth investigation into the carrier transport mechanism in the BCZT system is essential

ISSN No:-2456-2165 https://doi.org/10.38124/ijisrt/26jul270

to evaluate its potential for advanced high-temperature applications.

The present study aims to develop a non-lead ceramic exhibiting a phase transition at high temperature along with a high permittivity, thereby broadening its potential application range. In this context, the high-temperature electrical behavior of $Ba_{0.835}Ca_{0.165}Zr_{0.09}Ti_{0.91}O_3$ (abbreviated hereafter as BCZT4.5) ceramic has been investigated. To achieve this, comprehensive analyses have been conducted on the material's structural characteristics using X-ray diffraction (XRD), microstructural features via energy dispersive X-ray spectroscopy (EDS) and scanning electron microscopy (SEM), as well as its dielectric and AC electrical properties. Additionally, the study explores the underlying electrical conduction mechanism within the system.

II. EXPERIMENTAL PROCEDURE

The $Ba_{0.835}Ca_{0.165}Zr_{0.09}Ti_{0.91}O_3$ (BCZT4.5) ceramic powder was synthesized using the conventional mixed oxide process. The calcination and sintering conditions of BCZT4.5 were, respectively, kept at 1450°C/5 hours and 1500°C/3 hours in ambient air. Powder XRD data were recorded at 30°C using CuKα radiation across a wide 2θ range (15°–80°) to confirm the phase formation and crystallographic structure. Microstructural analysis, including SEM and EDS, was performed on the sintered pellet (fractured surface) using a field emission type scanning electron microscope (JEOL JSM-7600F, Japan) attached with EDS. For the dielectric measurements, platinum paste was applied to the polished ceramic surfaces to form electrodes. The real (ε') and imaginary (ε'') components of the permittivity were measured over a broad temperature range (50–850°C) and frequency span (1 Hz to 1 MHz) utilizing an Alpha high-resolution dielectric analyzer (Novocontrol Technologies).

III. RESULTS AND DISCUSSION

Fig. 1 presents the powder Rietveld-refined XRD profile of BCZT4.5 ceramics recorded at 30°C. The analysis affirms the single-phase forming of a tetragonal structure, indexed to the *P4/mmm* space group. The processed lattice parameters are determined to be a = 3.9967 Å and c = 3.9921 Å, yielding a unit cell volume of 63.7672 Å^3, with a goodness-of-fit parameter χ^2 = 2.65. It is well established that dielectric properties can vary significantly among capacitors due to even slight compositional differences, including those from different manufacturers.

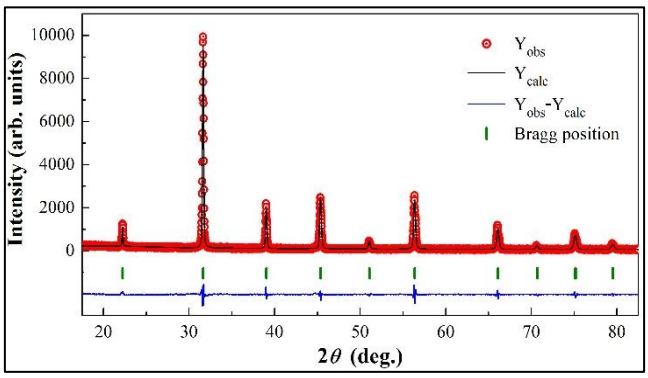

Fig 1 Room Temperature XRD Pattern of $Ba_{0.835}Ca_{0.165}Zr_{0.09}Ti_{0.91}O_3$ Ceramic.

The EDS spectrum, shown in Fig. 2(a), confirms the elemental composition of BCZT4.5, displaying only the expected peaks corresponding to Ba, Ca, Zr, Ti, and O, implying the compound's phase purity. Fig. 2(b) displays the SEM image of BCZT4.5 ceramics (fractured surface). The microstructure reveals a dense, polycrystalline texture with well-distributed grains with minimal porosity. The mean grain size was approximated to be approximately 6 µm, suggesting effective densification during sintering.

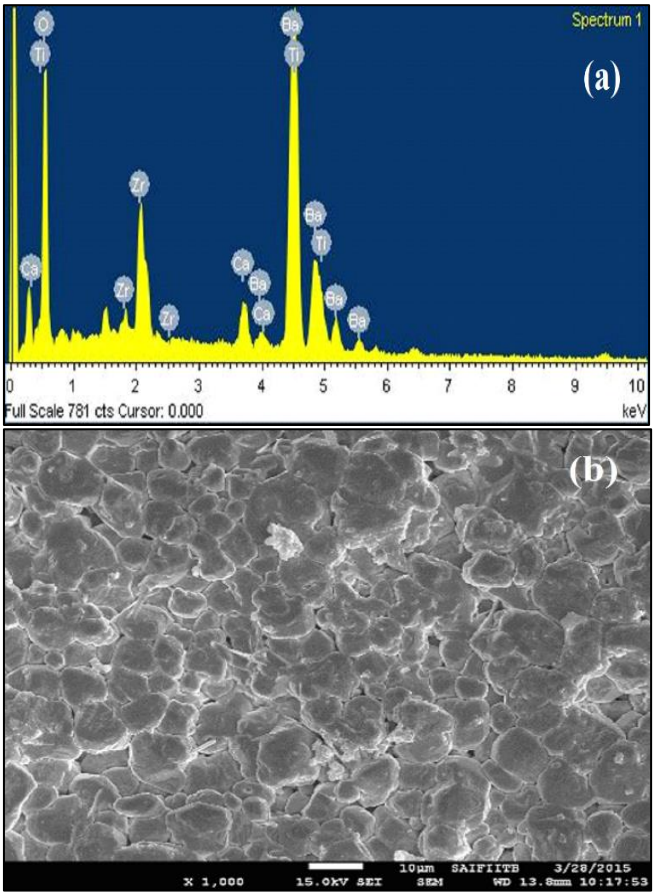

Fig 2 (a) EDS Spectrum and (b) SEM Micrograph of $Ba_{0.835}Ca_{0.165}Zr_{0.09}Ti_{0.91}O_3$ Ceramic.

The frequency-dependent variation of $\varepsilon'(f)$ and $\varepsilon''(f)$ at various temperatures is presented, respectively in Fig. 3 (a) and 3(b). It is noticed that ε' as well as ε'' both

ISSN No:-2456-2165 https://doi.org/10.38124/ijisrt/26jul270

follow inverse dependence on frequency except $\varepsilon''(f)$ at higher frequencies near room temperature, as expected for normal ferroelectrics. The observed dielectric relaxation behavior indicates that, within the operating frequency range, dipolar relaxation is largely masked by free charge carrier relaxation. Figs. 4(a) and 4(b) illustrate the temperature dependent variation of the ε' and ε'' across various frequencies. As depicted, both parameters initially decrease and then exhibit a rising trend with increasing temperature. This non-monotonic behavior suggests that the high value of the dielectric constant cannot be solely ascribed to extrinsic factors such as grain boundaries or grain size. Instead, intrinsic contributions, particularly those arising from localized electronic structure changes due to chemical substitution, are assumed to play a significant role. Additionally, the tangent loss ($\tan\delta = \varepsilon''/\varepsilon'$) is observed to cross zero, indicating the presence of a resonance phenomenon within the studied frequency range. This resonance behavior is especially pronounced at 800°C, as seen in the $\tan\delta$-f plot (Fig. 5a), where a sharp peak arises and shifts towards lower frequencies with increasing temperature. Fig. 5(b) further confirms the resonance effect in the $\tan\delta$-T plot at 1 MHz. It is well understood that the resonance effect defines the upper cutoff (limit) of usable frequency for a capacitor. Beyond the self-resonant frequency, the device begins to act as a DC-blocking inductor, where the reactance due to the inductive element (ωL) dominates over reactance due to capacitance, leading to a negative permittivity. This phenomenon is critical in high-speed electronics, where multilayer ceramic capacitors are usually employed as decoupling circuits and suppress high-frequency noise, particularly above the resonance frequency. Hence, minimizing the value of ωL is essential in such applications. Fig. 3(a), the inset displays a model equivalent circuit accounting for the effects of both resistance and inductance from the measurement setup. The total complex impedance of this system can be expressed accordingly as [28,29], where L and r_{el} represent the inductance and resistance of the leads and electrodes, respectively. The dielectric parameters for BCZT4.5 at room temperature and 1 kHz were measured to be: $\varepsilon' = 4351$, $\varepsilon'' = 65$, and $\tan\delta = 0.015$.

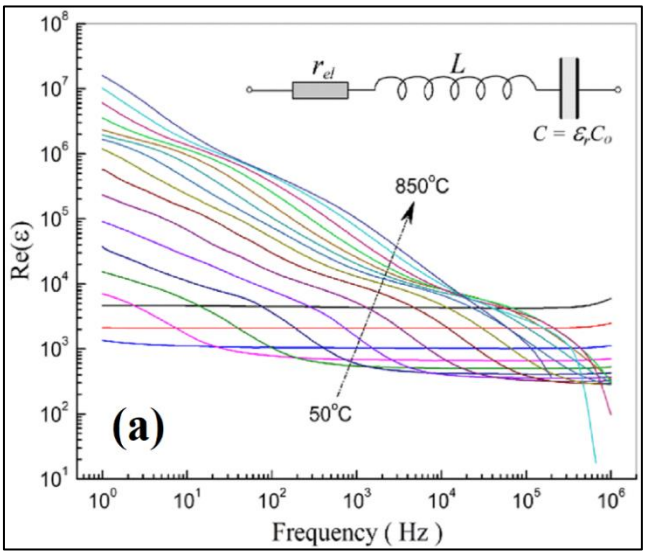

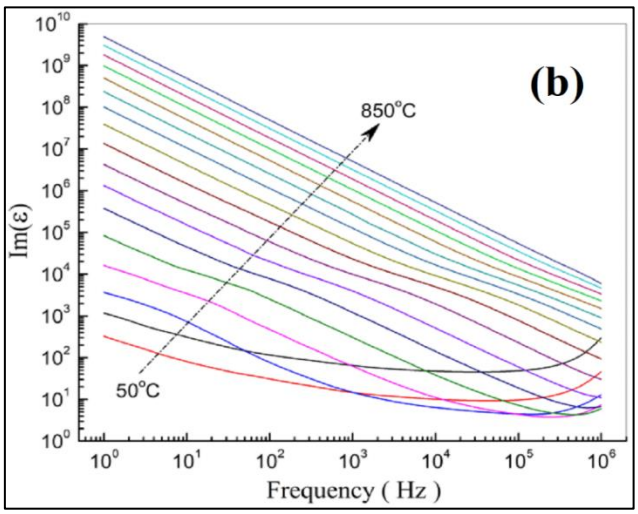

Fig 3 Frequency Dependent Variation of (a) ε' and (b) ε'' of $Ba_{0.835}Ca_{0.165}Zr_{0.09}Ti_{0.91}O_3$ Ceramic at Different Temperatures. Inset: Specified Capacitor Model for Frequency of Operation.

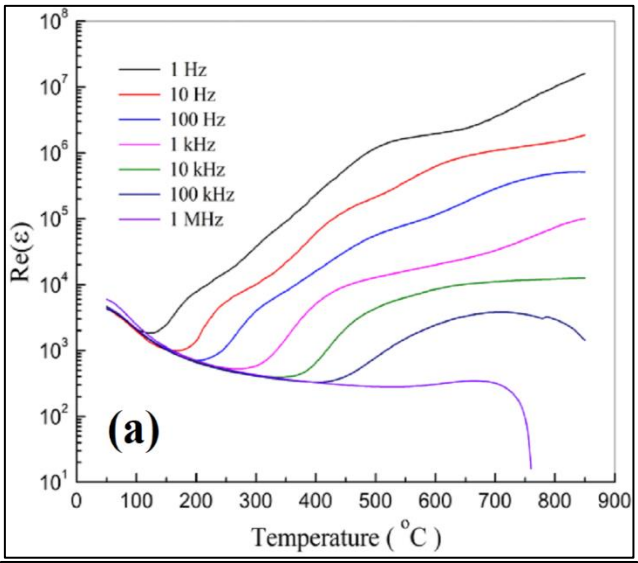

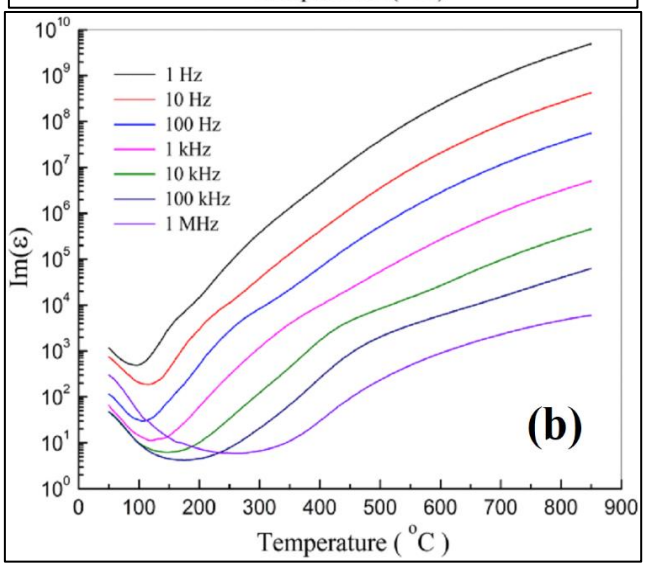

Fig 4 Temperature Dependent Variation of (a) ε' and (b) ε'' of $Ba_{0.835}Ca_{0.165}Zr_{0.09}Ti_{0.91}O_3$ Ceramic at Different Frequencies.

ISSN No:-2456-2165 https://doi.org/10.38124/ijisrt/26jul270

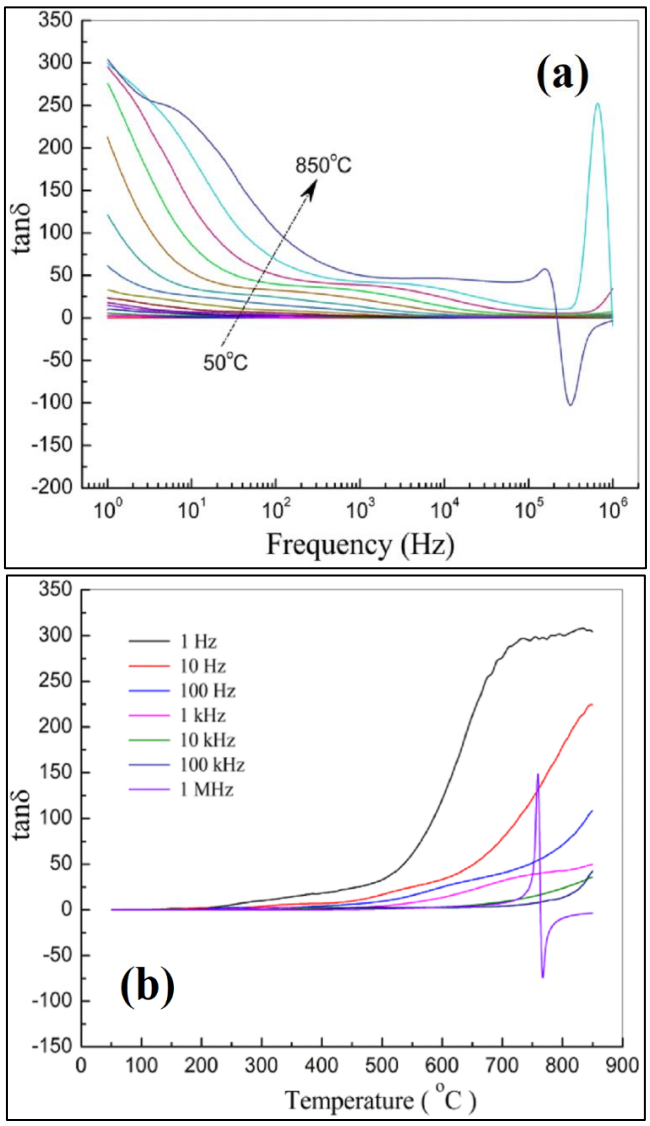

Fig 5 (a) Variation of Frequency-Dependent Tanδ at Different Temperatures and (b) Variation of Temperature-Dependent Tanδ at Different Frequencies of $Ba_{0.835}Ca_{0.165}Zr_{0.09}Ti_{0.91}O_3$ Ceramic.

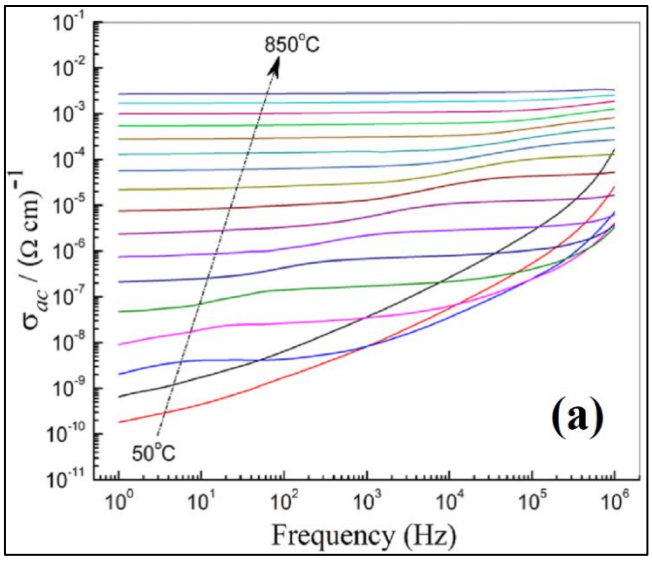

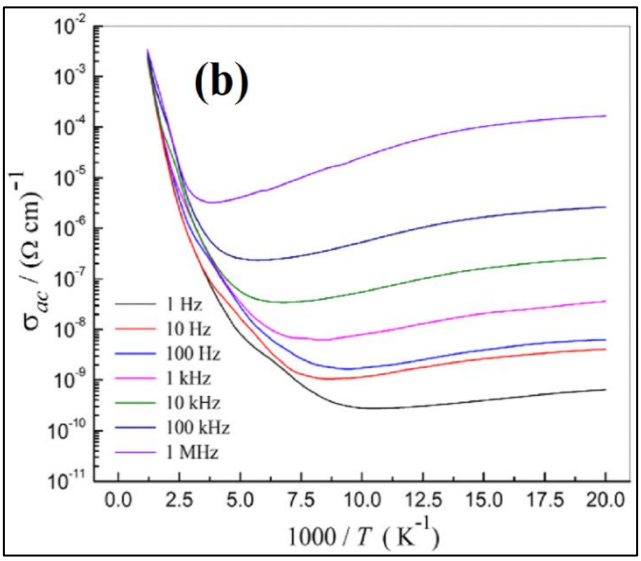

Fig 6 (a) Frequency Dependent Variation of σ_{ac} at Various Temperatures and (b) Temperature Dependent Variation of σ_{ac} at Various Frequencies of $Ba_{0.835}Ca_{0.165}Zr_{0.09}Ti_{0.91}O_3$ Ceramic.

The frequency-dependent AC conductivity (σ_{ac}) of BCZT4.5 at various temperatures is illustrated in Fig. 6(a). Across all temperatures, the conductivity spectra exhibit dispersion throughout the frequency range. As the frequency decreases, σ_{ac} values also decline and tend to become nearly frequency-independent (σ_{dc}), the DC component of conductivity, at higher temperatures. This behavior is attributed to the long-range translational motion of charge carriers, likely due to the presence of space charge within the material. The σ_{ac} versus frequency data follows a double power law expression: $\sigma_{ac} = \sigma_{dc} + A\omega^{S_1} + B\omega^{S_2}$. The exponent s_1 ($0 \leq s_1 \leq 1$) characterizes the low-frequency region, typically associated with grain boundary conductivity and translational ion hopping. Whereas, s_2 ($0 < s_2 < 2$) corresponds to the high-frequency region, indicating grain (bulk) conductivity, which suggests the presence of localized relaxation and/or ionic reorientation processes. The activation energy in this context is linked to the reorientation of ions during hopping [30]. According to the jump relaxation model (JRM), ions may either successfully transition to a new site or return to their original site (unsuccessful hop). If the surrounding lattice relaxes around the ion's new position, the hop becomes successful, contributing to conductivity in the low-frequency region. Further, at higher frequencies, the probability of unsuccessful hops increases, resulting in the observed frequency-dependent dispersion in conductivity. It is known that in perovskite-type oxides, charge traps commonly exist within the bandgap, influencing conduction. The JRM implies that different activation energies are associated with successful and unsuccessful hopping events. From the data, s_1 reaches a maximum value of approximately 0.9, while s_2 peaks near 1.2 and consistently exceeds 1.

Fig. 6(b) displays the temperature dependence (plotted as $10^3/T$) of $\log \sigma_{ac}$ at various frequencies. The conduction activation energy was calculated applying the Arrhenius

ISSN No:-2456-2165 https://doi.org/10.38124/ijisrt/26jul270

relation: $\sigma_{ac} = \sigma_o \exp(-E_a / k_B T)$. A least-squares (linear) fit to this equation in the high-temperature region yields the apparent activation energy (E_a), which is found to increase with frequency; from 0.66 eV at 1 Hz to 0.68 eV at 1 MHz. Furthermore, the increase in conductivity with rising temperature can be attributed to the formation of oxygen vacancies during sintering, leading to charge imbalance. This process is described by the Kröger-Vink notation: $O_o \rightarrow \frac{1}{2}O_2 \uparrow + V_o^{\bullet\bullet} + 2e^{-1}$. This indicates that free electrons are generated, suggesting BCZT4.5 to be n-type. Besides, the temperature- and frequency-dependent variation of σ_{ac} in BCZT4.5 is consistent with hopping-type charge transport and aligns well with the dictates of the jump relaxation model.

IV. CONCLUSIONS

The non-lead ceramic composition $Ba_{0.835}Ca_{0.165}Zr_{0.09}Ti_{0.91}O_3$ was synthesized via the conventional mixed-oxide route and was confirmed to have a tetragonal perovskite structure with *P*4/*mmm* space group. The microstructural analysis revealed an average grain size of ~6 μm. The ceramic displayed a high dielectric permittivity value of 4351 and a low tangent loss of 0.015 at room temperature and 1 kHz. The dielectric capacitor demonstrated a resonance frequency above 0.66 MHz at 800°C that shifted to around 0.16 MHz at 850°C, influenced by variations in its capacitance. AC conductivity measurements indicated that charge transport in the material follows a hopping mechanism consistent with the jump relaxation model, having an apparent activation energy of 0.66 eV at 1 Hz. The ceramic system's high dielectric constant paired with a low dielectric loss ($\sim 10^{-2}$) highlights its promise as a viable lead-free candidate for capacitor applications.

ACKNOWLEDGMENT

Authors are thankful to SAIF, IIT Bombay, Mumbai for providing the XRD data and SEM micrographs.

REFERENCES

[1]. X. Jiang, K. Kim, S. Zhang, J. Johnson, and G. Salazar, "High-temperature piezoelectric sensing," Sensors, 14, pp. 144-169, 2014.

[2]. Z. Wang, X. M. Chen, L. Ni, Y. Y. Liu, and X. Q. Liu, "Dielectric relaxations in $Ba(Fe_{1/2}Ta_{1/2})O_3$ giant dielectric constant ceramics," Appl. Phys. Lett., 90, pp. 102905, 2007.

[3]. S. Zhang, and F. Yu, "Piezoelectric materials for high-temperature sensors," J. Am. Ceram. Soc., 94, pp. 3153-3170, 2011.

[4]. D. Damjanovic, "Materials for high-temperature piezoelectric transducers," Curr. Opin. Solid State Mater. Sci., 3, pp. 469-473, 1998.

[5]. R. Kažys, A. Voleišis, and B. Voleišienė, "High-temperature ultrasonic transducers: Review," Ultragarsas, 63, pp. 7-17, 2008.

[6]. C.-M. Lin, T.-T. Yen, V.V. Felmetsger, M.A. Hopcroft, J. H. Kuypers, and A.P. Pisano, "Thermally compensated aluminum nitride Lamb wave resonators for high-temperature applications," Appl. Phys. Lett., 97, pp. 083501, 2010.

[7]. S. Zhang, Y. Zheng, H. Kong, J. Xin, E. Frantz, and T. R. Shrout, "Characterization of high-temperature piezoelectric crystals with an ordered langasite structure," J. Appl. Phys., 105, pp. 114107, 2009.

[8]. S. Zhang, Y. Fei, B. H. Chai, E. Frantz, D. W. Snyder, X. Jiang, and T. R. Shrout, "Characterization of piezoelectric single crystal $YCa_4O(BO_3)_3$ for high-temperature applications," Appl. Phys. Lett., 92, pp. 202905, 2009.

[9]. G. W. Hunter, J. D. Wrbanek, R. S. Okojie, P. G. Neudeck, G. C. Fralick, L. Chen, J. Xu, and G. M. Beheim, "Development and application of high-temperature sensors and electronics for propulsion applications," Proc. SPIE 6222, Sensors for Propulsion Measurement Applications, pp. 622209, 2006.

[10]. F. Yu, S. Zhang, X. Zhao, D. Yuan, L. Qin, Q. -M. Wang, and T. R. Shrout, "Dielectric and electromechanical properties of rare earth calcium oxyborate piezoelectric crystals at high-temperatures," IEEE Trans. Ultrason. Ferroelectr. Freq. Control, 58, pp. 868, 2011.

[11]. S. Zhang, Y. Fei, E. Frantz, D. Snyder, B. Chai, and T. R. Shrout, "High-temperature piezoelectric single crystal $ReCa_4O(BO_3)_3$ for sensor applications," IEEE Trans. Ultrason. Ferroelectr. Freq. Control, 55, pp. 2703, 2008.

[12]. M. Acosta, J. Zang, W. Jo, and J. Rödel, "High-temperature dielectrics in $CaZrO_3$-modified $Bi_{1/2}Na_{1/2}TiO_3$-based lead-free ceramics," J. Euro. Ceram. Soc., 32, pp. 4327, 2012.

[13]. R. Dittmer, W. Jo, D. Damjanovic, and J. Rödel, "Lead-free high-temperature dielectrics with wide operational range," J. Appl. Phys., 109, pp. 034107, 2011.

[14]. J.B. Lim, S. Zhang, N. Kim, and T.R. Shrout, "High-temperature dielectrics in the $BiScO_3$–$BaTiO_3$–$K_{0.5}Bi_{0.5}TiO_3$ ternary system," J. Am. Ceram. Soc., 92, pp. 679, 2009.

[15]. T. Zheng, and J. Wu, "Enhanced piezoelectric activity in high-temperature $Bi_{1-x-y}Sm_xLa_yFeO_3$ lead-free ceramics," J. Mater. Chem. C, 3 pp. 3684, 2015.

[16]. I.P. Raevski, S.A. Prosandeev, A.S. Bogatin, M.A. Malitskaya, and L. Jastrabik, "High dielectric permittivity in $AFe_{1/2}B_{1/2}O_3$ nonferroelectric perovskite ceramics (A=Ba, Sr, Ca; B=Nb, Ta, Sb)," J. Appl. Phys., 93, pp. 4130, 2003.

[17]. C.-Y. Chung, Y.H. Chang, and G.J. Chen, "Effect of lanthanum doping on the dielectric properties of $Ba(Fe_{0.5}Nb_{0.5})O_3$ ceramic," J. Appl. Phys., 96, pp. 6624, 2004.

[18]. C.C. Homes, T. Vogt, S.M. Shapiro, S. Wakimoto, and A.P. Ramirez, "Optical response of high-dielectric-constant perovskite-related oxide," Science, 293, pp. 673, 2001.

[19]. S. Bhagat, and K. Prasad, "Structural and impedance spectroscopy analysis of $Ba(Fe_{1/2}Nb_{1/2})O_3$ ceramic," Phys. Status Solidi A, 207, pp. 1232, 2010.

[20]. A.R. West, T.B. Adams, F.D. Morrison, and D.C. Sinclair, "Novel high capacitance materials: $BaTiO_3$:

ISSN No:-2456-2165 https://doi.org/10.38124/ijisrt/26jul270

La and $CaCu_3Ti_4O_{12}$," J. Euro. Ceram. Soc., 24, pp. 1439, 2004.
[21]. T.-T. Fang, and H.-K. Shiau, "Mechanism for developing the boundary barrier layers of $CaCu_3Ti_4O_{12}$," J. Am. Ceram. Soc., 87, pp. 2072, 2004.
[22]. L. Zhang, "Electrode and grain-boundary effects on the conductivity of $CaCu_3Ti_4O_{12}$," Appl. Phys. Lett., 87, pp. 022907, 2005.
[23]. C.C. Wang, and L.W. Zhang, "Surface-layer effect in $CaCu_3Ti_4O_{12}$," Appl. Phys. Lett., 88, pp. 042906, 2006.
[24]. L. Ni, X.M. Chen, X.Q. Liu, and R.Z. Hou, "Microstructure-dependent giant dielectric response in $CaCu_3Ti_4O_{12}$ ceramics," Solid State Commun., 139, pp. 45, 2006.
[25]. S.M. Ke, H.T. Huang, and H.Q. Fan, "Relaxor behavior in $CaCu_3Ti_4O_{12}$ ceramics," Appl. Phys. Lett., 89, pp. 182904, 2006.
[26]. W. Liu, and X. Ren, "Large piezoelectric effect in Pb-free ceramics," Phys. Rev. Lett., 103, pp. 257602, 2009.
[27]. K.P. Chandra, R. Singh, A.R. Kulkarni, and K. Prasad, "High temperature phase diagram of pseudo binary $Ba(Zr_{0.2}Ti_{0.8})O_3$-$(Ba_{0.7}Ca_{0.3})TiO_3$ ceramic system: *In situ* X-ray diffraction and dielectric studies," Ferroelectr., 514, pp. 105, 2017.
[28]. K.P. Chandra, A.R. Kulkarni, and K. Prasad, "On the high temperature phase transition in $Ba(Zr_{0.20}Ti_{0.80})O_3$ ceramic," J. Adv. Dielectr., 7, pp. 1750025, 2017.
[29]. K.P. Chandra, Rajan Singh, A.R. Kulkarni, and K. Prasad, "High temperature phase transition in $(Ba_{0.76}Ca_{0.24})(Zr_{0.04}Ti_{0.96})O_3$ ceramic," Ferroelectr., 502, pp. 231, 2016.
[30]. C.R. Bowen, and D.P. Almond, "Modelling the `universal' dielectric response in heterogeneous materials using microstructural electrical networks," Mater. Sci. Technol., 22, pp. 719, 2006.